Proc. Natl. Acad. Sci. USA
Vol. 93, pp. 9545–9552, September 1996
Cell Biology

This contribution is part of the special series of Inaugural Articles by members of the National Academy of Sciences elected on April 25, 1995.

Cross talk between cell death and cell cycle progression: BCL-2 regulates NFAT-mediated activation

GERALD P. LINETTE*, YING LI*, KEVIN ROTH, AND STANLEY J. KORSMEYER†

Howard Hughes Medical Institute and Division of Molecular Oncology, Departments of Medicine and Pathology, Washington University School of Medicine, St. Louis, MO 63110

Contributed by Stanley J. Korsmeyer, July 17, 1996

ABSTRACT **BCL-2-deficient T cells demonstrate accelerated cell cycle progression and increased apoptosis following activation. Increasing the levels of BCL-2 retarded the $G_0 \rightarrow S$ transition, sustained the levels of cyclin-dependent kinase inhibitor $p27^{Kip1}$, and repressed postactivation death. Proximal signal transduction events and immediate early gene transcription were unaffected. However, the transcription and synthesis of interleukin 2 and other delayed early cytokines were markedly attenuated by BCL-2. In contrast, a cysteine protease inhibitor that also blocks apoptosis had no substantial affect upon cytokine production. Interleukin 2 expression requires several transcription factors of which nuclear translocation of NFAT (nuclear factor of activated T cells) and NFAT-mediated transactivation were impaired by BCL-2. Thus, select genetic aberrations in the apoptotic pathway reveal a cell autonomous coregulation of activation.**

Homeostasis of cell numbers requires a carefully orchestrated balance between input (proliferation) and output (cell death) processes. Important questions remain as to how these two reactions are coordinated to achieve a remarkably invariant number of cells within each lineage. One thesis would hold that two independent genetic pathways exist that control cellular proliferation or cell death. In this scenario, balance would be attained by communication with extracellular cues. This includes the well-documented competition between cells for limited survival factors in their surrounding microenvironment (1). Incontrovertible evidence now exists for a distinct genetic pathway controlling programmed cell death. The *Bcl-2* protooncogene isolated from the chromosomal breakpoint of t(14;18) bearing B cell lymphoma (2–4) serves as a repressor of apoptosis in mammalian cells (5–7). Gain of function studies that overexpressed wild-type *Bcl-2* extended survival rather than promoting proliferation and lead to an excess of lymphocytes that eventually progressed to B and T cell malignancy (8–10). Loss of function analysis that knocked out the *Bcl-2* or *Bcl-x_L* death repressor resulted in the loss of cells from selected lineages (11–13). While hematopoietic lineages appear to develop normally in the *Bcl-2*-deficient mice, they display a striking inability to maintain homeostasis of lymphocytes with apoptotic loss of B and T cells.

While established gene products clearly regulate apoptosis, it is unclear whether they have roles that affect other pathways. A second thesis would argue that a balanced population of cells would be difficult to maintain unless a cell autonomous coordination existed between decisions to divide and decisions to die. A number of experimental models argue that improper activation and aberrant cell cycle progression can prompt individual cells to initiate suicide. For example, overexpression of *Myc* in the absence of serum results in apoptosis (14). This has been envisioned as signaling a conflict or perhaps the dual capacity of *Myc* as a transcription factor to initiate a death as well as a proliferation program (15). Mice deficient in a cell cycle regulator, the retinoblastoma gene product (*Rb*), demonstrate abnormal mitotic figures as well as death of embryonic neurons (16, 17). In parallel, the overexpression of *E2F*, which mimics *Rb* deficiency, can also result in apoptosis (18, 19). From this perspective, there would appear to be a capacity to identify aberrations in proliferation that would trigger the apoptotic elimination of dangerous cells.

We chose to approach this complex issue from the opposite perspective, asking whether regulators of cell death impact the cellular proliferation pathway. To pursue this, we elected to contrast genetic models of *Bcl-2* loss-of-function (lf) and *Bcl-2* transgenic gain-of-function (gf) using cells from these mice that were otherwise normal. *Bcl-2* homozygous knockout (−/−), heterozygous (+/−), wild-type (+/+), and lck^{pr}-*Bcl-2* transgenics (which overexpress wild-type protein, also referred to as *Bcl-2* gf) provide a gradient of BCL-2 levels within T cells (10, 11). Thus, any effects upon activation and proliferation noted in *Bcl-2* gf cells would be considerably strengthened by an opposite effect in *Bcl-2* lf cells. We selected T cells as a representative model of resting, G_0, mature cells with distinct stages of transition between $G_0 \rightarrow S$ phase. T cells require BCL-2 to maintain homeostasis, and a well-defined signal transduction pathway interconnects the T cell surface antigen receptor to cell cycle regulators (20). Steps can be separated into mitogenesis in which proximal signal transduction events lead to immediate early gene expression during the transition from $G_0 \rightarrow G_1$ and into a later critical event in mid G_1 phase in which the expression and signaling by interleukin 2 (IL-2), a physiologic growth factor, are required for progression into S phase (21).

MATERIALS AND METHODS

Cell Preparations and Culture. Single cell suspensions were prepared from spleen or thymus and erythrocytes were lysed in 0.17 M NH_4Cl for 10 min at 4°C. Splenic T cells were purified by negative selection with immunomagnetic beads as described except that incubation of cells with magnetic beads was performed for 1 hr at 4°C (22). T cells were always 90–95% pure as judged by CD3 staining and were >95% viable. Freshly isolated splenic T cells were cultured in 24-well plates (Costar) in 1 ml complete media (Iscove's medium containing 10% heat-inactivated FCS, 100 units/ml penicillin, 50 units/ml streptomycin, 1 mM Hepes, and 5×10^{-5} M 2-mercaptoethanol) at 37°C, 5% CO_2/95% oxygen. Splenic T cells were stimulated in 24-well plates coated with anti-CD3 mAb.

Abbreviations: lf, loss-of-function; gf, gain-of-function; IL, interleukin; RT-PCR, reverse transcription–PCR; PMA, phorbol 12-myristate 13-acetate; cdk, cyclin-dependent kinase.

*G.P.L. and Y.L. are co-first authors as they contributed equally to this work.

†To whom reprint requests should be addressed.

Briefly, protein-A purified anti-mouse CD3 mAb (145–2C11, PharMingen) was diluted in 0.05 M Tris (pH 9.3) in a volume of 250 μl and allowed to absorb overnight at 4°C. Afterwards, wells were washed twice and 3–5 × 10^5 T cells in a volume of 1 ml complete medium were added to individual wells. When indicated, anti-murine CD28 mAb (23) (PV-1, a gift from C. June, Naval Medical Research Institute) (24) was added in fluid phase at a final concentration of 5 μg/ml. Jurkat T cell line (25) (E6-1 clone, American Type Culture Collection) was transfected with SFFV-human *Bcl-2* or control plasmid SFFV-neo. Stably transfected Jurkat cells were selected in G418 and characterized and monitored for expression of human BCL-2 protein by fluorescence-activated cell sorter and Western blot analysis with the 6C8 mAb (7). Jurkat cells were stimulated with solid phase anti-human CD3 mAb (HIT3a, PharMingen) and phorbol 12-myristate 13-acetate (PMA) 10 ng/ml (Sigma) in RPMI 1640 complete media containing 10% FCS.

Cell Cycle Analysis. Stimulated T cells were harvested, washed twice in cold PBS, and lysed in Krishan's reagent (0.05 mg/ml propidium iodide/0.1% sodium citrate/0.02 mg/ml ribonuclease A/0.3% Nonidet P-40). Cell nuclei were then analyzed at low flow rate for DNA content based on FL-2A versus FL-2W linear plots on a FACscan (Becton Dickinson) using CELLFIT or CELLQUEST software. In several experiments, cell cycle analysis of S-phase distribution was confirmed with BrdU incorporation (26).

Reverse Trascription–PCR (RT-PCR). Total RNA was isolated from activated T cells using the acid quanidium thiocyanate phenol-chloroform extraction method (RNAzol). One microgram RNA was reverse transcribed (RT Superscript, GIBCO) with random hexamers to generate cDNA (20 μl) for each time point. Two microliters of each cDNA mixture was amplified with 0.5 units *Taq* polymerase (Perkin–Elmer) using specific oligonucleotide primers (27). Preliminary experiments were performed to determine the optimal number of cycles for quantitative determination of each reaction product under the conditions of annealing at 60°C (1 min), extension at 72°C (1 min), and denaturing at 94°C (1 min) using a Perkin–Elmer Thermocycler. One tenth of each reaction mixture was electrophoresed on 4–20% polyacrylamide gels (NOVEX, San Diego) in 1× TBE at 100 volts; RT-PCR products were transferred to 0.45 u nylon membrane in 0.5× TBE at 200 mA for 1 hr. Nylon membranes were probed with ^{32}P-end-labeled internal oligonucleotides at 42°C for 16–24 hr. Membranes were washed and exposed in the linear range of x-ray film (Kodak).

Electrophoretic Mobility-Shift Assay. Nuclear extracts from 5 × 10^7 Jurkat cells stimulated with anti-CD3 mAb solid phase and 20 ng/ml PMA in T75 culture flasks were prepared as described (28). Protein concentrations were determined by the Bio-Rad protein assay. Electrophoretic mobility-shift assay was performed as described (29). Binding reactions were done with 2.5 μg protein in the 10 mM Tris·HCl (pH 7.5), 50 mM NaCl, 0.5 mM EDTA, 5% glycerol, 10 μg BSA, and 1 μg poly(dI·dC) in a volume of 20 μl. The binding reactions were incubated at room temperature for 20 min (AP-1) or 30 min [NFAT (nuclear factor of activated T cells), NFκB, OCT-1] with 0.2–0.4 ng double-stranded oligonucleotide. Gel-purified double-stranded oligonucleotides were end-labeled with [γ-^{32}P]ATP (Amersham) using T4 kinase. Oligonucleotides for human NFAT, NFκB, AP-1, and OCT-1 (28, 29) containing monomer binding sites were used. The samples were electrophoresed in native 6% polyacrylamide gels in 0.5% TBE at 100 V.

Confocal Microscopy. Both Jurkat/neo and Jurkat/Bcl-2 cells were fixed and permeabilized with 4% paraformaldehyde and methanol. Anti-NFATc3 polyclonal antibody and fluorescein-conjugated goat anti-rabbit IgG were used to stain NFATc3. Nuclei were counterstained by propidium iodide. Confocal laser scanning was performed using a Sarastro 2000 confocal laser scanning microscope (Molecular Dynamics) and IMMAGE SPACE software (Molecular Dynamics).

Transient Transfection and Luciferase Assay. Jurkat cells (10^7) were transiently transfected by electroporation (960 μF, 250 V) with 10 μg of NFAT-luciferase or AP-1-luciferase reporter DNA. Eighteen hours after transfection, cells were activated with 300 ng/ml anti-CD3 plus 10 ng/ml PMA. A number of cells (10^6) per each condition were harvested at 6 hr after activation for AP-1 or 24 hr for NFAT reporter constructs, and assayed for luciferase activity (Luciferase Assay System, Promega).

RESULTS

BCL-2 Influences Thymocyte Cell Cycle. To assess the effect of BCL-2 on cell cycle progression, thymocytes from *Bcl-2*$^{-/-}$, *Bcl-2*$^{+/-}$, *Bcl-2*$^{+/+}$, and lck^{pr}-*Bcl-2* transgenic mice (gf) were pulsed with 10 μM BrdU for 1 hr at 37° in 10% FCS stained with anti-BrdU-fluorescein isothiocyanate and counterstained with propidium iodide. Similar to prior studies, 8.1% of *Bcl-2*$^{+/+}$ (wild-type) thymocytes were in S phase (Fig. 1*A*). However, more thymocytes were consistently in cycle as BCL-2 levels fell in *Bcl-2*$^{+/-}$ and *Bcl-2*$^{-/-}$ mice 9.1% and 9.5%, respectively, in the examples shown here. Most strikingly, overexpressed BCL-2 resulted in a marked decrease of thymocytes in S phase, only 1.5% in the *Bcl-2* gf mouse (Fig. 1*A*).

BCL-2 Levels Determine Cell Volume of Resting T Cells. Peripheral T cells are in the G_0 phase of the cell cycle before activation. Cell volume represents one further measurement of the relative state of quiescence. The *Bcl-2*$^{-/-}$, *Bcl-2*$^{+/-}$, *Bcl-2*$^{+/+}$, and *Bcl-2* gf genotypes displayed stepwise increments of BCL-2 protein in purified splenic T cells (10). We noted that BCL-2 levels dictated T cell size as measured by forward scatter (linear scale) on flow cytometry (Fig. 1*B*). In the experiment shown, the forward scatter of *Bcl-2*$^{-/-}$ cells was 456 mean channel unites, while the forward scatter of *Bcl-2*$^{+/+}$ T cells was 421. In contrast, T cells from lck^{pr}-*Bcl-2* transgenic mice were the smallest with a forward scatter of 336. Similar results were obtained when cell volume was determined by a Coulter Counter (data not shown).

BCL-2 Determines the Duration of G_0 → S Phase. T cells from the *Bcl-2* genetic models were used to assess the role of BCL-2 upon activation-induced cell cycle progression. The time course of mitogenesis as measured by the time for stimulated T cells to enter S phase proved proportional to the level of BCL-2. Peripheral T cells from individual mice were stimulated with plate bound (solid phase) anti-CD3 monoclonal antibody (mAb) and were analyzed for DNA content by propidium iodide staining at serial time points. *Bcl-2* gf T cells showed a marked delay of entry into S phase after activation when compared with *Bcl-2*$^{+/+}$ T cells. Conversely, *Bcl-2*$^{-/-}$ T cells entered S phase more rapidly than normal (Fig. 2*A*). For example, at 24 hr postactivation, 32% of *Bcl-2*$^{-/-}$, 22% of *Bcl-2*$^{+/-}$, 9% of *Bcl-2*$^{+/+}$, but only 3% of *Bcl-2* gf T cells were in S + G_2/M phase based upon >2N DNA content. To determine if *Bcl-2* could still regulate cells activated through multiple signal transduction pathways, T cells were costimulated with anti-CD28 mAb as well as with anti-CD3. As previously noted, addition of anti-CD28 mAb to T cells stimulated with optimal concentrations of anti-CD3 has a small, additional affect on cell cycle progression (30) (Fig. 2*B*). At 24 hr postactivation, 35% of *Bcl-2*$^{-/-}$, 27% of *Bcl-2*$^{+/-}$, 15% of *Bcl-2*$^{+/+}$, and yet only 6% of *Bcl-2* gf T cells were determined to be in S + G_2/M. Thus, BCL-2 had a similar affect upon the kinetics of G_0 → S phase transition following costimulation.

BCL-2 Also Affects Activation Induced Cell Death. Forty-eight hours after stimulation, the percent of cells in S + G_2/M phases decreased in *Bcl-2*-deficient T cells, but was still increasing in T cells overexpressing *Bcl-2* (Fig. 2 *A* and *B*). This suggested that there may be differences in viability that follow activation. To evaluate this, T cells that were stimulated with anti-CD3 mAb were assessed for apoptotic cells, which reside in the population with <2N DNA content. Immediately after

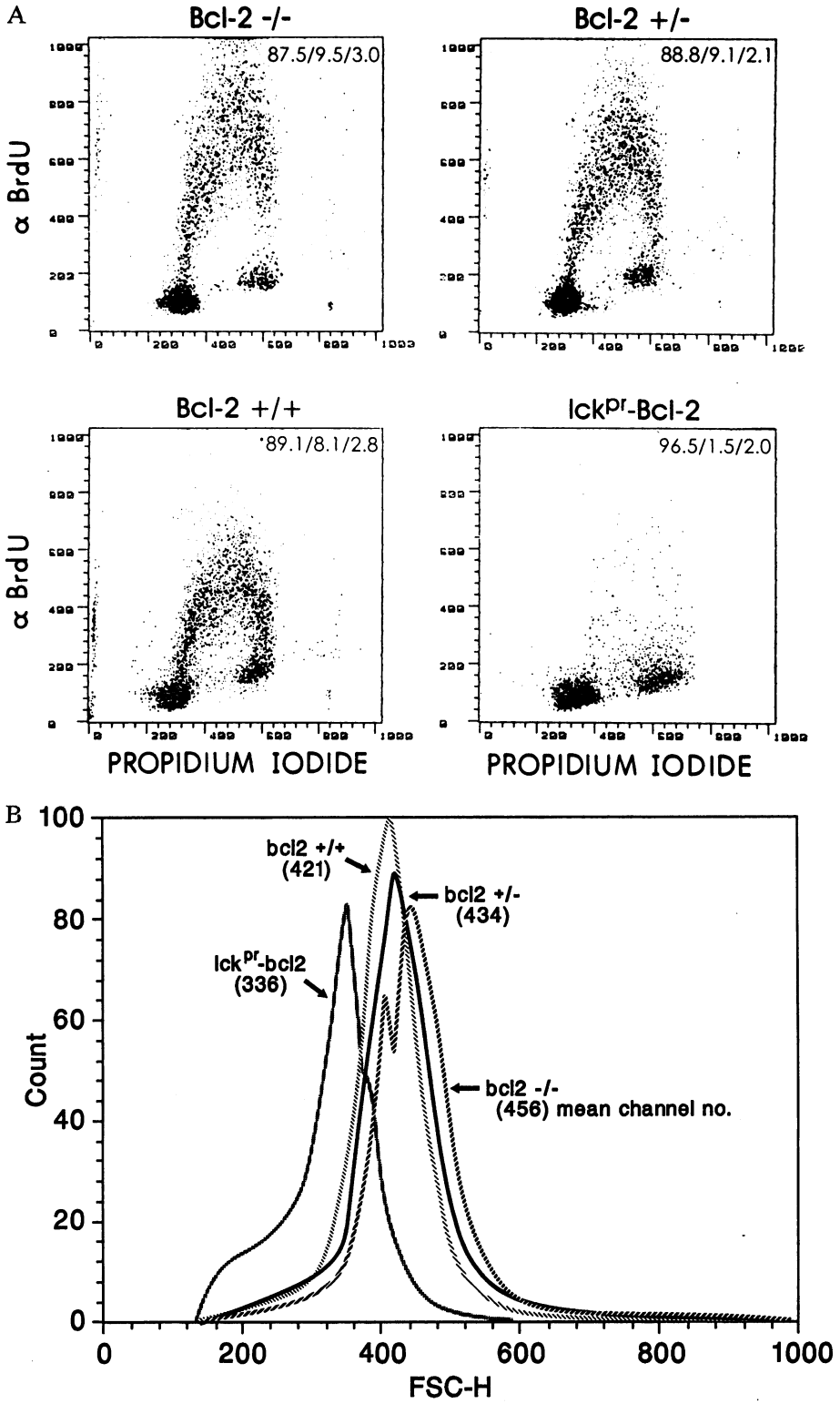

FIG. 1. BCL-2 affects cell cycle and cell size. (*A*) Thymocytes from healthy 5-week-old *Bcl-2*$^{-/-}$, *Bcl-2*$^{+/-}$, and *Bcl-2*$^{+/+}$ littermates as well as an lck^{pr}-*Bcl-2* transgenic mouse were incubated with BrdU, washed and developed with an anti-BrdU-FITC antibody. Propidium iodide staining was performed just before analysis by flow cytometry. The percentage of Cells in G_0 + G_1/S/G_2 + M phase is shown in the upper right corner of each dot plot. (*B*) The mean forward scatter (linear scale) of CD3 positive T cells from each mouse (7 weeks of age) was determined on a FACscan with CELLQUEST software. Purified splenic T cells were >95% CD3 positive. Results are representative of three experiments.

purification, less than 1% of T cells from each mouse (*Bcl-2*$^{-/-}$, *Bcl-2*$^{+/+}$, and *Bcl-2* gf) were apoptotic. After anti-CD3 activation, *Bcl-2*$^{-/-}$ T cells demonstrated accelerated cell death as well as premature cell cycle progression (Fig. 2*C*). For example, at 24 hr, 27% of *Bcl-2*$^{-/-}$ versus 12% of *Bcl-2*$^{+/+}$, but only 7% of *Bcl-2* gf T cells were apoptotic. *Bcl-2*$^{-/-}$ cells continued to show an increased percentage of dying (17%) as well as proliferating cells (33%) at 36 hr. Even after 48 hr, most *Bcl-2* gf T cells remained in G_0/G_1 with only 8% apoptotic and 15% proliferating cells. These differential results were confirmed by

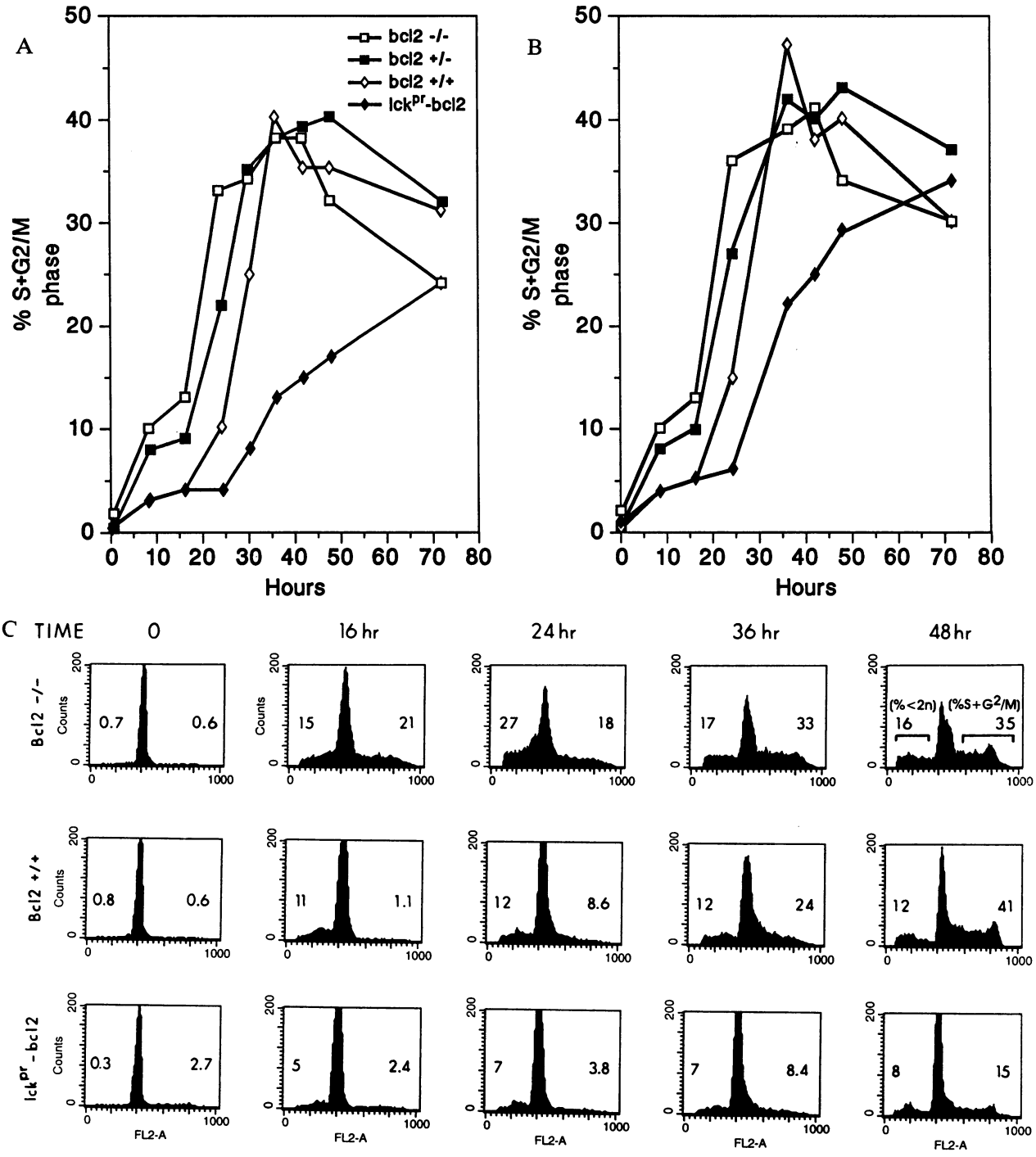

FIG. 2. BCL-2 regulates the $G_0 \rightarrow S$ transition. Purified T cells were activated with anti-CD3 mAb (500 ng per well solid phase) (*A*) or in combination with anti-CD28 mAb, PV-1 (5 μg/ml fluid phase added at time 0) (*B*). At serial time points, cells from individual wells were harvested and analyzed for DNA content after gating out apoptotic cells (<2N DNA content) and debris. A total of 10,000 events were collected and cells with >2N DNA content were determined to be in S + G_2/M phase. Results are representative of 10 independent experiments. (*C*) Purified T cells stimulated with anti-CD3 mAb were studied for DNA content by propidium iodide staining and flow cytometry. Only small debris was gated out, such that apoptotic nuclei were also included in this analysis. The percent apoptotic (<2N) and proliferating cells (>2N: S + G_2/M) is indicated. Results are representative of three independent experiments.

TUNEL (TdT-mediated dUTP-biotin nick end labeling) (31), which proved more sensitive than propidium iodide in detecting apoptotic cells (not shown).

Regulation of $p27^{Kip1}$ but Not p21 Is Altered by BCL-2. The retarded entry of *Bcl-2* gf T cells into S phase was accompanied by a delayed pattern of retinoblastoma hyperphosphorylation (data not shown). A prominence of underphosphorylated Rb was also recently noted in *Bcl-2* gf thymocytes (32). $p27^{Kip1}$ (33, 34) and p21 (also known as *cip1*, *sdi*, *waf1*, and *cap20*) (35, 36) are cyclin-dependent kinase (cdk) inhibitors present in T cells. In resting mature T cells, $p27^{Kip1}$ is present at significant levels. Upon activation, p27 protein is degraded during early-to-mid G_1 phase, presumably mediated by IL-2 signaling (37, 38). Conversely, resting T cells possess minimal amounts of p21, but upon activation p21 levels increase in G_1. *Bcl-2*$^{+/-}$ T cells show an accelerated disappearance of $p27^{Kip1}$ protein after anti-CD3 activation, relative to *Bcl-2*$^{+/+}$ T cells (Fig. 3). This contrasts with a delayed loss of $p27^{Kip1}$ in *Bcl-2* gf T cells. The

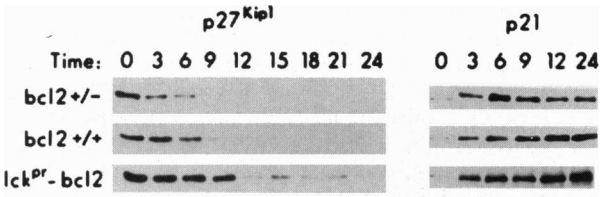

FIG. 3. $p27^{Kip1}$ but not p21 levels are affected by BCL-2. Western blot analysis of $p27^{Kip1}$ and p21 in T cells stimulated with anti-CD3 mAb (500 ng per well solid phase) at serial time points. Protein (10 μg) in each lane was run on SDS/12% polyacrylamide gels, transferred to nitrocellulose, and blotted either with a polyclonal rabbit anti-p27 Ab (Santa Cruz 1 μg/ml) or with a mAb to p21 (a gift from J. Wade Harper, Baylor College of Medicine). Blots were developed with Enhanced Chemiluminesence (Amersham). The $p27^{Kip1}$ results have been confirmed in two additional experiments.

relative amounts of $p27^{Kip1}$ in T cells of each *Bcl-2* genotype correlates well with the duration of the $G_0 \rightarrow S$ phase transition. In contrast, BCL-2 had no striking effect upon the regulation of p21 (Fig. 3).

Proximal Signal Transduction and Immediate Early Gene Responses Appear Unaffected by BCL-2. The level of cell surface TCR/CD3 complex did not vary among the T cells of various *Bcl-2* genotypes (data not shown). This indicated that the effect of BCL-2 upon T cell activation would reside between proximal signal transduction events and distal cell cycle machinery. Dissection of this pathway revealed that the pattern of tyrosine phosphorylated proteins was similar in activated T cells of the various *Bcl-2* genotypes. Similarly, the rise in intracellular ionized calcium concentrations following activation of T cells or thymocytes was comparable (data not shown).

The time course of immediate early gene induction in response to TCR/CD3 activation was assessed. The induction of *c-Myc* RNA was detectable at 30 min postactivation and remained elevated at 1, 2, and 6 hr in T cells of all four *Bcl-2* genotypes (Fig. 4*A*). Other immediate early genes (*c-Fos*, *c-Jun*, *NGFI-B*) were also induced to a similar degree in each *Bcl-2* genotype. These data indicate that proximal signal transduction events through immediate early gene transcription were not strongly influenced by BCL-2.

BCL-2 Regulates IL-2 Production by Activated T Cells. Most cytokines produced by T cells, including IL-2, display a temporal time course typical of delayed early response genes. IL-2 is produced by activated T cells and acts as the primary progression factor in mid G_1 phase for T cell proliferation. *Bcl-2* gf T cells produced substantially less (≈5-fold) IL-2 compared with *Bcl-2*$^{+/+}$ T cells at optimal concentrations of anti-CD3 antibody, (i.e., 100 and 1000 ng per well) (Fig. 5*A*). Of interest, *Bcl-2*$^{+/-}$ and *Bcl-2-/-* T cells produced greater amounts of IL-2 and even produced IL-2 following suboptimal (i.e., 10 ng per well) concentrations of anti-CD3 mAb (Fig. 5*A*). Costimulation of T cells with anti-CD28 mAb as well as anti-CD3 mAb can enhance IL-2 production (as well as other cytokines) (30). When T cells from all groups were activated with an optimal concentration (1000 ng per well) of anti-CD3, the addition of anti-CD28 mAb produced approximately 4- to 5-fold more IL-2 (Fig. 5*B*). However, increasing amounts of BCL-2 protein proportionally depressed the IL-2 response to costimulation as well (Fig. 5*B*).

To determine if the influence of BCL-2 operated at the level of cytokine transcription, RT-PCR analysis of *IL-2* and two other T cell-derived cytokines, *IL-3* and *GM-CSF*, was performed. The induction of *IL-2*, *IL-3*, and *GM-CSF* RNA was quite delayed in *Bcl-2* gf T cells when compared with *Bcl-2*$^{+/+}$ cells (Fig. 4*B*). Consistent with the data in Fig. 5*A*, *Bcl-2*$^{-/-}$ T cells showed accelerated transcription of *IL-2*, *IL-3*, and *GM-CSF* (Fig. 4*B*).

BCL-2 but Not Cysteine Protease Inhibitors Block Cytokine Production in Jurkat T Cells. To further examine the interrelationship amongst BCL-2, cell cycle progression, and *IL-2*

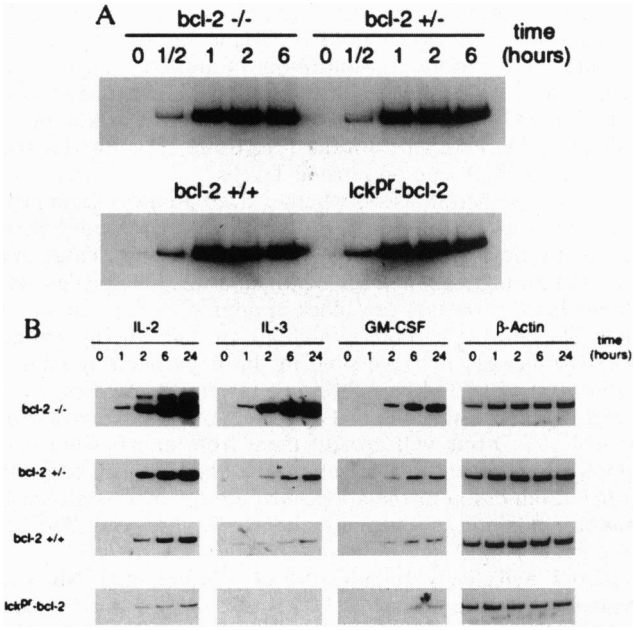

FIG. 4. *Bcl-2* alters cytokine RNA induction but not immediate early genes. (*A*) Induction of c-myc in T cells is unaffected by BCL-2. Purified T cells (2×10^6) were activated with anti-CD3 (500 ng per well solid phase) for 0.5, 1, 2, and 6 hr, and total RNA was isolated. Products of a quantitative RT-PCR assay were transferred to nitrocellulose and hybridized with a ^{32}P-radiolabeled mouse *c-Myc* fragment. RT-PCR of β-actin confirmed that comparable amounts of RNA were present in each sample (*B*). (*B*) Cytokine RNA induction in activated T cells is modulated by BCL-2. RNA samples from *A* were assessed by quantitative RT-PCR using oligonucleotide primers for murine *IL-2* (28 cycles), *IL-3* (32 cycles), *GM-CSF* (32 cycles), and β-actin (24 cycles). PCR products were transferred to nitrocellulose and hybridized with a ^{32}P-end-labeled oligonucleotide probe internal to each set of primers. This result is representative of three independent experiments.

transcription, a T cell line model was established. Jurkat is a well-characterized human T cell leukemia line used principally to study activation events and *IL-2* regulation (25). Jurkat cells were stably transfected with *Bcl-2* and expressed ≈10-fold

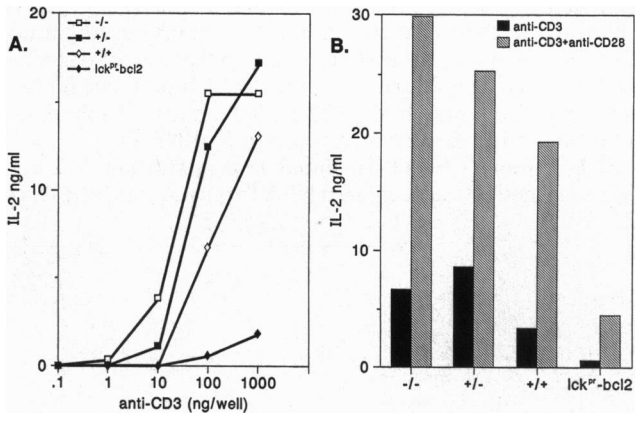

FIG. 5. BCL-2 regulates IL-2 production in activated T cells. (*A*) Purified T cells (1×10^6) were cultured in plates coated with 10-fold dilutions of anti-CD3 mAb. After 24 hr, cell-free supernatants were assayed for murine IL-2 using a capture ELISA with mAb pairs (PharMingen). Each 1.0 ml culture supernatant (100 μl) was assayed and the mean of triplicate determinations (SD <10%) is shown. This experiment was performed three times with similar results and was confirmed using a CTLL-2 proliferation assay. (*B*) Cells (1×10^6) were activated with anti-CD3 mAb (1000 ng per well solid phase) or in combination with anti-CD28 mAb (5 μg/ml fluid phase). After 26 hr at 37°C, supernatants were assayed for IL-2. Values plotted are the mean of triplicate determinations (SD <15%). This experiment was repeated with similar results.

more BCL-2 protein when compared with parental Jurkat cells as determined by flow cytometry (data not shown). When activated with various concentrations of anti-CD3 plus PMA, Jurkat/*Bcl-2* cells produce substantially less IL-2. Production of IL-3 and GM-CSF is also markedly reduced in Jurkat/*Bcl-2* cells (Fig. 6). Thus, the Jurkat T cell line recapitulates the effects of BCL-2 seen on normal T cells.

We next wished to assess whether decreased cytokine production was a generalized affect that followed any inhibition of the apoptotic pathway. The ICE-like cysteine proteases are required for programmed cell death, and small molecules that inhibit these proteases can block apoptosis. A peptide-based molecule, benzoxy carbonyl-Val-Ala-Asp-fluoromethylketone (zVAD-fmk), is an irreversible inhibitor particularly potent against the CPP32-like subset of cysteine proteases. Our previous studies indicated that treatment of Jurkat T cells with 50 μM zVAD-fmk will protect them from anti-Fas-induced apoptosis and block the activation of CPP32 (39). In contrast to *Bcl-2*, inhibition of the apoptotic pathway by this protease inhibitor did not substantially alter *IL-2*, *IL-3*, or *GM-CSF* production (Fig. 6).

BCL-2 Selectively Impairs NFAT Binding and Nuclear Translocation. NFAT, AP-1, NFκB, and OCT-1 are all transcription factors required for optimal IL-2 transcription (20). To assess the effect of BCL-2 upon their binding activity, Jurkat cells were activated with anti-CD3 plus PMA and nuclear extracts were prepared and tested by electrophoretic mobility-shift assay. Interestingly, NFAT binding activity from activated Jurkat/*Bcl-2* cells was substantially diminished when compared with Jurkat/neo cells (Fig. 7*A*). Other inducible factors tested including AP-1 and NFκB did not appear to be substantially affected by BCL-2. Likewise, OCT-1, a constitutive octamer binding protein, remained unaffected by the expression of BCL-2 (Fig. 7*A*).

The localization of NFATc3 ($NFAT_x$) (40) within Jurkat T cells was assessed with a laser-scanning confocal microscope. An antibody recognizing NFATc3 revealed it was predominantly in the cytosol of either unstimulated Jurkat or unstimulated Jurkat/*Bcl-2* T cells (Fig. 7*B*). Eight hours after activation, the NFATc3 in Jurkat cells was essentially absent from the cytosol and was predominantly present in clustered aggregates within the nucleus. In contrast, NFAT remained prominent in the cytosol of Jurkat/*Bcl-2* cells and the NFAT present within the nucleus displayed a more finely dispersed pattern (Fig. 7*B*). Western blot analysis indicated that the total level of NFATc3 was comparable in unstimulated Jurkat and Jurkat/*Bcl-2* cells (data not shown). Thus, *Bcl-2* markedly alters the activation-induced nuclear translocation of NFAT.

BCL-2 Inhibits NFAT-Mediated Transactivation. We next assessed whether the decreased NFAT translocation and DNA binding activity manifested as impaired NFAT-mediated gene transcription. Jurkat/neo and Jurkat/Bcl-2 cells were transiently transfected either with the NFAT-luciferase construct or with a control AP-1-luciferase construct (29). Transfected Jurkat cells were subsequently activated with anti-CD3 plus PMA and assayed for luciferase activity. AP-1-mediated transcriptional activation was comparable in both the activated Jurkat/neo and Jurkat/Bcl-2 cells (Fig. 8). In contrast, the presence of BCL-2 resulted in up to a 40-fold suppression of NFAT-mediated transactivation (Fig. 8).

DISCUSSION

Bcl-2 genetic models of altered cell death provide evidence for a cell autonomous coordination between apoptosis and cell cycle progression. A gradient of BCL-2 levels revealed a linear relationship between the susceptibility to activation and the vulnerability to death. The level of BCL-2 dictated the duration of $G_0 \rightarrow S$ phase transition with a critical point of regulation at the mid G_1 phase dependence upon IL-2 synthesis and signaling (Fig. 9). Mazel *et al.* (32) also recently noted a delay in the S phase transition of *Bcl-2* transgenic cells when compared with wild type. The classical measurements of mitogenesis and of $G_0 \rightarrow G_1$ transition were not strongly influenced by BCL-2. Proximal signal transduction events including tyrosine phosphorylation and mobilization of Ca^{2+} were quite similar whatever the BCL-2 level. Expression of immediate early genes including *Myc, Fos, Jun*, and *NGF-IB* is a classic criterion for $G_0 \rightarrow G_1$ phase transition, but was not altered by BCL-2.

The most dramatic effect of BCL-2 upon T cell activation was focused at the production of IL-2 in mid G_1 phase. The transcription of *IL-2* was the most definable point of cross talk between BCL-2 and activation (Fig. 9). Optimal expression of *IL-2* requires three inducible transcription factors, NFAT, AP-1, and NFκB. Any of these three might have been responsible as prior studies (these are provided below as each is detailed) have implicated each in affecting cell death. FOS, which forms heterodimers with JUN to constitute AP-1, is expressed after a variety of death stimuli (41). *NFκB* appears to be regulated by redox and has also been implicated in regulating cell death (42). NFAT is a transcription factor supracomplex composed of distinct nuclear and cytoplasmic subunits that act in concert to permit DNA binding and transcriptional activation (40, 43, 44).

NFAT-mediated *IL-2* transcription is complex. NFATp/c rapidly translocates to the nucleus after Ca^{2+} signaling, an event blocked by cyclosporin A and hence requiring the action of the phosphatase PP2B, calcineurin (45, 46). The ability of BCL-2 to inhibit NFAT DNA binding and impair NFAT-mediated gene transcription identifies it as a principal site of BCL-2's influence. The marked decrease in the nuclear translocation of NFAT in

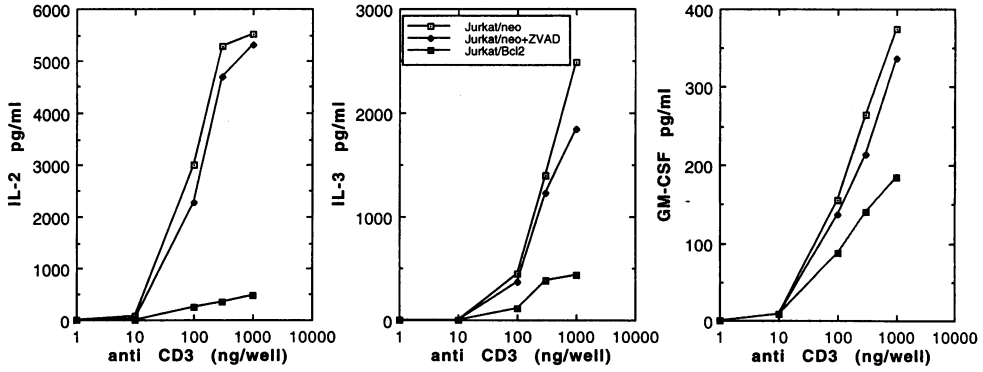

FIG. 6. BCL-2 but not zVAD-fmk impairs production of IL-2, IL-3, and GM-CSF in Jurkat cells. Cells (1×10^6) of bulk stably transfected Jurkat T cell lines were stimulated with anti-CD3 mAb (1000 ng per well solid phase) plus PMA 10 ng/ml in 1 ml complete media. zVAD-fmk was added to Jurkat/neo at 50 μM. After 24 hr at 37°C, cell-free supernatants were subjected to one freeze thaw, and assayed for each cytokine using a capture ELISA (R & D Systems). Each point is the mean of triplicate determinations (SD <10%) for IL-2, IL-3, or GM-CSF.

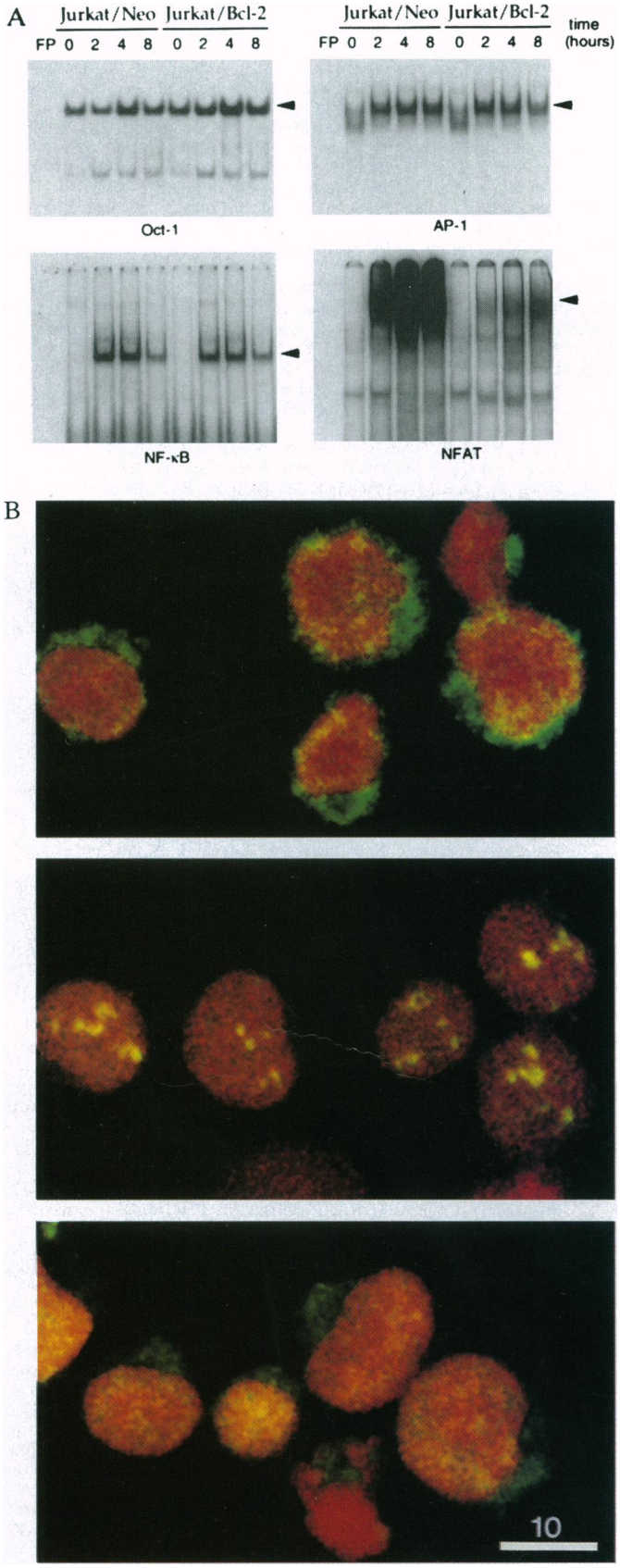

FIG. 7. Bcl-2 impairs NFAT DNA binding and nuclear translocation. (*A*) Jurkat cells (≈5 × 10^5 per ml) were stimulated in T75 culture flasks coated with optimal concentrations of anti-CD3 mAb plus PMA for various times (0, 2, 4, and 8 hr). Nuclear extracts were prepared and gel-shift analysis performed with 2.5–5 μg protein extract and radiolabeled DNA probes on 6% native polyacrylamide gels in 0.5× TBE. Bands were judged to be specific (indicated by arrows) based on competition analysis with cold oligonucleotides and supershift with antibodies specific for each transcription factor (data not shown). FP, free probe. (*B*) Immuofluorescent confocal microscopy of Jurkat cells using anti-NFATC3 polyclonal antibody. An unstimulated Jurkat/Bcl-2 clone (*Top*) was indistinguishable from unstimulated Jurkat/neo (data not shown); Jurkat/neo cells stimulated with anti-CD3 mAb plus PMA for 8 hr (*Middle*) are compared with stimulated Jurkat/Bcl-2 cells at 8 hr (*Bottom*).

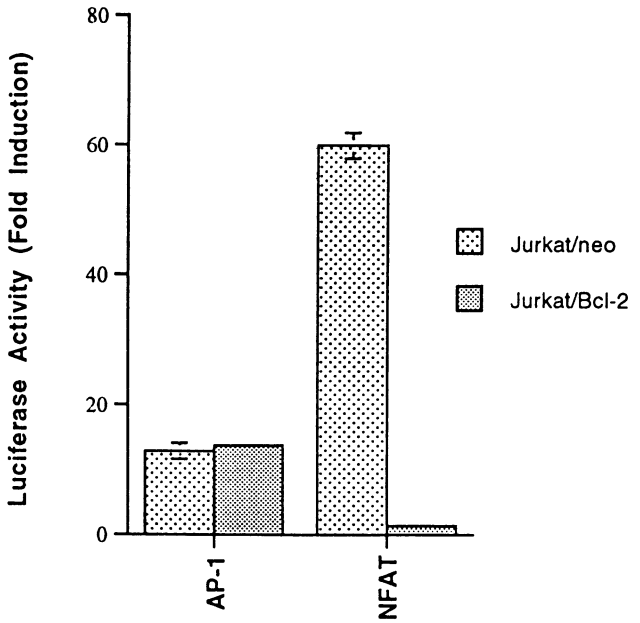

FIG. 8. BCL-2 impairs NFAT-mediated transactivation. Jurkat/neo and Jurkat/Bcl-2 clones were transiently transfected either with a NFAT-luciferase reporter or with an AP-l-luciferase reporter construct. After stimulation with anti-CD3 plus PMA, 10^6 cells were harvested and assayed for luciferase activity. Results are expressed as the mean fold induction from three independent assays measuring luciferase activity in stimulated over unstimulated cells.

BCL-2-expressing cells suggests this step as a major site of BCL-2 regulation. Inhibition of calcineurin by CsA/cyclophilin or FK506/FKBP indicates that it is critical to regulating IL-2 and other cytokines. NFAT has been implicated in TCR/CD3-mediated cell death and CsA can inhibit this apoptotic pathway in T cell hybridomas (47). One possibility is that NFAT induces a death program as well as a proliferation program. While IL-2 regulation by NFAT is a clearly defined site of BCL-2 impact upon activation, others could exist. Other cytokine responses, IL-3 and GM-CSF, were also abnormal yet also require NFAT (43). Adding exogenous IL-2 to BCL-2-expressing T cells only corrected about half of the activation deficit. This may reflect the delay in IL-2Rα, CD25 expression also noted in BCL-2 overexpressing cells (data not shown). Evidence that a rapamycin-sensitive intracellular IL-2 signaling pathway leads to *Bcl-2* gene induction has recently been noted (48) and might represent a feedback control system.

The level of BCL-2 had a selective impact upon the cdk inhibitor $p27^{Kip1}$, but not p21. Recent evidence indicates that IL-2 signaling correlates with a transition in cell cycle control from the $p27^{Kip1}$ to the p21 cdk inhibitor (37, 38). The cdk inhibitors are felt to interconnect proximal signal transduction events with regulation of the cdks that phosphorylate substrates including retinoblastoma and thus regulate cell cycle (49, 50). Normally, IL-2 signaling leads to the inactivation of $p27^{Kip1}$, allowing cdk activation and subsequent progression through G_1 into S phase. The more rapid loss of $p27^{Kip1}$ in *Bcl-2* lf cells and its retention in *Bcl-2* gf cells may follow from the altered IL-2 production.

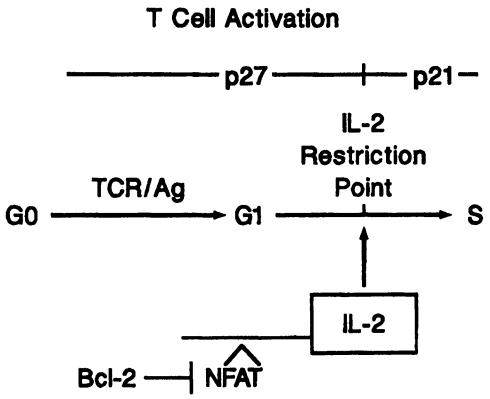

FIG. 9. Schematic representation of a site of BCL-2's affect upon activation.

However, we cannot formally exclude a primary effect of BCL-2 upon a cdk inhibitor such as $p27^{Kip1}$. The influence of BCL-2 upon $G_0 \rightarrow S$ transition and upon p27 but not p21 fits well with the emerging data that p27 may regulate cdk activity from quiescence to S phase, while p21 may be more restricted to regulating cdk function in cycling cells (38).

Prior studies noted little effect of BCL-2 on doubling time as long as factor-dependent cells were continuously proliferating in the presence of IL-3. However, when cells were returned to G_0 by IL-3 deprivation, the time required to return to S phase following readdition of IL-3 was lengthened by BCL-2 (51, 52). The shortened $G_0 \rightarrow S$ phase transition time in *Bcl-2* lf cells described here argues that the delays noted with *Bcl-2* gf are a primary event rather than an artifact of damaged cells that avoided death. Moreover, the inability of a cysteine protease inhibitor to alter cytokine production also favors a selective role for *Bcl-2* rather than a secondary effect following inhibition of apoptosis.

What would be the teleologic advantage of communication between cell death and cell cycle pathways? Postactivation apoptosis accompanied the accelerated cell cycle progression of *Bcl-2*-deficient cells. This is reminiscent of the fulminant lymphoid apoptosis noted in *Bcl-2*$^{-/-}$ mice (11). However, even healthy appearing *Bcl-2* knockouts display a progressive decline in peripheral T and B cells over time. As a correlate, T cell cultures that are not stimulated (media with 10% FCS) also demonstrated increased death of *Bcl-2*$^{-/-}$ cells (data not shown). Thus, BCL-2 loss leads to immunodeficiency both from an apparently shorter half-life of resting cells and from a susceptibility to postactivation-induced death. In contrast, excess BCL-2 leads to hyperplasia and would be expected to save cells with acquired mutations that would otherwise be destined to die. In this context, it was surprising that the incidence of malignancies was relatively low (12–30%) and had a long latency (1–1.5 years) in *Bcl-2* transgenic mice (8–10). The growth disadvantage of *Bcl-2*-overexpressing cells as noted here would help explain this paradox. Excess BCL-2 would suppress the outgrowth and accumulation of such death resistant cells. A cell autonomous interrelationship between cell death and cell cycle programs would provide the tightest regulation to ensure both balanced homeostasis and cancer surveillance.

G.P.L. and Y.L. contributed equally to this work. We are grateful to Dr. Gerald Crabtree for generously providing luciferase expression constructs, NFATc3 Ab, and helpful discussions. We also thank Dr. Carl June in whose laboratory the $[Ca^{2+}]$ measurements were performed with the assistance of Doug Smoot. We thank Gary Brown for animal husbandry and Mary Pichler for expert preparation of this manuscript. This work was supported by National Cancer Institute Grant CA 49712.

1. Raff, M. C. (1992) *Nature (London)* **356,** 397–400.
2. Tsujimoto, Y., Gorham, J., Cossman, J., Jaffe, E. & Croce, C. M. (1985) *Science* **229,** 1390–1393.
3. Bakhshi, A., Jensen, J. P., Goldman, P., Wright, J. J., McBride, O. W., Epstein, A. L. & Korsmeyer, S. J. (1985) *Cell* **41,** 899–906.
4. Cleary, M. L. & Sklar, J. (1985) *Proc. Natl. Acad. Sci. USA* **82,** 7439–7443.
5. Vaux, D. L., Cory, S. & Adams, J. M. (1988) *Nature (London)* **335,** 440–442.
6. McDonnell, T. J., Deane, N., Platt, F. M., Nuñez, G., Jaeger, U., McKearn, J. P. & Korsmeyer, S. J. (1989) *Cell* **57,** 79–88.
7. Hockenbery, D. M., Nuñez, G., Milliman, C., Schreiber, R. D. & Korsmeyer, S. J. (1990) *Nature (London)* **348,** 334–336.
8. McDonnell, T. J. & Korsmeyer, S. J. (1991) *Nature (London)* **349,** 254–256.
9. Strasser, A., Harris, A. W. & Cory, S. (1993) *Oncogene* **8,** 1–9.
10. Linette, G. P., Hess, J. L., Sentman, C. L. & Korsmeyer, S. J. (1995) *Blood* **86,** 1255–1260.
11. Veis, D., Sorenson, C. M., Shutter, J. R. & Korsmeyer, S. J. (1993) *Cell* **75,** 229–240.
12. Ma, A., Pena, J. C., Chang, B., Margosian, E., Davidson, L., Alt, F. W. & Thompson, C. B. (1995) *Proc. Natl. Acad. Sci. USA* **92,** 4763–4767.
13. Motoyama, N., Wang, F., Roth, K., Sawa, H., Nakayama, K., Nakayama, K., Negishi, I., Senju, S. & Loh, D. Y. (1995) *Science* **267,** 1506–1510.
14. Evan, G. I., Wyllie, A. H., Gilbert, C. S., Littlewood, T. D., Land, H., Brooks, M., Waters, C. M., Penn, L. Z. & Hancock, D. C. (1992) *Cell* **69,** 119–128.
15. Harrington, E. A., Bennett, M. R., Fanidi, A. & Evan, G. I. (1994) *EMBO J* **994,** 3286–3295.
16. Lee, E. Y.,-H. P., Chang, C. Y., Hu, N., Wange, Y.-C. J., Lai, C.-C., Herrup, K., Lee, W.-H. & Bradley, A. (1992) *Nature (London)* **359,** 288–294.
17. Jacks, T., Fazeli, A., Schmitt, E. M., Bronson, R. T., Goodell, M. A. & Weinberg, R. A. (1992) *Nature (London)* **359,** 295–300.
18. Shan, B. & Lee, B.-H. (1994) *Mol. Cell. Biol.* **14,** 8166–8173.
19. Qin, X.-Q., Livingston, D. M., Kaelin, W. G. & Adams, P. D. (1994) *Proc. Natl. Acad. Sci. USA* **91,** 10918–10922.
20. Fraser, J. D., Strauss, D. & Weiss, A. (1993) *Immunol. Today* **14,** 357–362.
21. Pardee, A. B. (1989) *Science* **246,** 603–608.
22. Linette, G. P., Grusby, M. J., Hedrick, S. M., Hansen, T. H., Glimcher, L. H. & Korsmeyer, S. J. (1994) *Immunity* **1,** 197–205.
23. Abe, R., Vandenberghe, P., Craighead, N., Smoot, D. S., Lee, K. P. & June, C. H. (1995) *J. Immunol.* **154,** 985–997.
24. June, C. H., Fletcher, M. C., Ledbetter, J. A. & Samelson, L. E. (1990) *J. Immunol.* **144,** 1591–1599.
25. Weiss, A. & Stobo, J. D. (1994) *J. Exp. Med.* **160,** 1284–1299.
26. Carayon, P. & Bord, A. (1992) *J. Immunol. Methods* **147,** 225–230.
27. Montgomery, R. A. & Dallman, M. J. (1991) *J. Immunol.* **147,** 554–560.
28. Fiering, S., Northrop, J. P., Nolan, G. P., Mattila, P. S., Crabtree, G. R. & Herzenberg, L. A. (1990) *Genes Dev.* **4,** 1823–1834.
29. Mattila, P. S., Ullman, K. S., Fiering, S., Emmel, E. A., McCutcheon, M., Crabtree, G. R. & Herzenberg, L. A. (1990) *EMBO J.* **9,** 4425–4433.
30. Thompson, C. B., Lindsten, T., Ledbetter, J. A., Kunkel, S. L., Young, H. A., Emerson, S. G., Leiden, J. M. & June, C. H. (1989) *Proc. Natl. Acad. Sci. USA* **86,** 1333–1337.
31. Gavrieli, Y., Sherman, Y. & Ben-Sasson, S. A. (1992) *J. Cell Biol.* **119,** 493–501.
32. Mazel, S., Burtrum, D. & Petrie, H. T. (1996) *J. Exp. Med.* **183,** 2219–2226.
33. Polyak, K., Lee, M.-H., Erdjument-Bromage, H., Koff, A., Roberts, J. M., Tempst, P. & Massagué, J. (1994) *Cell* **78,** 59–66.
34. Toyoshima, H. & Hunter, T. (1994) *Cell* **78,** 67–74.
35. Harper, J. W., Adami, G. R., Wei, N., Keyomarsi, K. & Elledge, S. J. (1993) *Cell* **75,** 805–816.
36. El-Deiry, W. S., Tokino, T., Velculescu, V. E., Levy, D. B., Parsons, R., Trent, J. M., Lin, D., Mercer, W. E., Kinzler, K. W. & Vogelstein, B. (1993) *Cell* **75,** 817–825.
37. Firpo, E. J., Koff, A., Solomon, M. J. & Roberts, J. M. (1994) *Mol. Cell. Biol.* **14,** 4889–4901.
38. Nourse, J., Firpo, E., Flanagan, W. M., Coats, S., Polyak, K., Lee, M.-H., Massague, J., Crabtree, G. R. & Roberts, J. M. (1994) *Nature (London)* **372,** 570–573.
39. Armstrong, R. C., Aja, T., Xiang, J., Gaur, S., Krebs, J., Hoang, K., Bai, X, Korsmeyer, S. J., Karanewsky, D. S., Fritz, L. C. & Tomaselli, K. J. (1996) *J. Biol. Chem.* **271,** 16850–16855.
40. Ho, S. N., Thomas, D. J., Timmerman, L. A., Li, X., Francke, V. & Crabtree, G. R. (1995) *J. Biol. Chem.* **270,** 19898–19907.
41. Smeyne, R. J., Vendrell, M., Hayward, M., Baker, S. J., Miao, G. G., Schilling, K., Robertson, L., Curran, T. & Morgan, J. I. (1993) *Nature (London)* **363,** 166–169.
42. Baeuerle, P. A. & Henkel, T. (1994) *Annu. Rev. Immunol.* **12,** 141–179.
43. Rao, A. (1994) *Immunol. Today* **15,** 274–281.
44. Crabtree, G. R. & Clipstone, N. A. (1994) *Annu. Rev. Biochem.* **63,** 1045–1083.
45. O'Keefe, S. J., Tamura, J., Kincaid, R. L., Tocci, M. J. & O'Neill, E. A. (1992) *Nature (London)* **357,** 692–694.
46. Clipstone, N. A. & Crabtree, G. R. (1992) *Nature (London)* **357,** 695–697.
47. Fruman, D. A., Burakoff, S. J. & Bierer, B. E. (1994) *FASEB J.* **8,** 391–400.
48. Miyazaki, T., Liu, Z.-J., Kawahara, A., Minami, Y., Yamada, K., Tsujimoto, Y., Barsoumian, E. L., Perlmutter, R. M. & Taniguchi, T. (1995) *Cell* **81,** 223–231.
49. Weinberg, R. A. (1995) *Cell* **81,** 323–330.
50. Sherr, C. J. & Roberts, J. M. (1995) *Genes Dev.* **9,** 1149–1163.
51. Nunez, G., London, L., Hockenbery, D., Alexander, M., McKearn, J. P. & Korsmeyer, S. J. (1990) *J. Immunol.* **144,** 3602–3610.
52. Marvel, J., Perkins, G. R., Rivas, A. L. & Collins, M. K. L. (1994) *Oncogene* **9,** 1117–1122.